

## Multi-Polarization SAR Change Detection: Unstructured Versus Structured GLRT

Vincenzo Carotenuto, Carmine Clemente,  
Antonio De Maio, John J. Soraghan and Salvatore Iommelli

V. Carotenuto, A. De Maio and S. Iommelli are with University of Napoli "Federico II"  
C. Clemente and J. J. Soraghan are with University of Strathclyde

*September, 9<sup>th</sup>, 2014, Sensor Signal Processing For Defence, SSPD 2014, Edinburgh, UK*



# Contents

- 1 Introduction
- 2 Problem Formulation
- 3 Unstructured and Structured GLRT
- 4 Performance Assessment
- 5 Conclusions

## Introduction

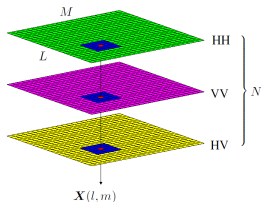
- Change detection is the capability to identify temporal changes within a given scene starting from a pair of co-registered images representing the area of interest;
- Two main approaches exist: incoherent and coherent;
- We introduce a structured approach to derive the Generalized Likelihood Ratio Test;
- The block diagonal structure of the polarimetric covariance matrix is exploited to achieve our goal, moreover the derived rule shows Constant False Alarm Rate (CFAR) behavior.

## Problem Formulation

1/2

A multipolarization SAR sensor measures for each pixel of the image under test  $N \in \{2, 3\}$  complex returns, collected from different polarimetric channels.

The  $N$  returns from the same pixel are stacked to form the vector  $\mathbf{X}(l, m)$ , where  $l = 1, \dots, L$  and  $m = 1, \dots, M$ .

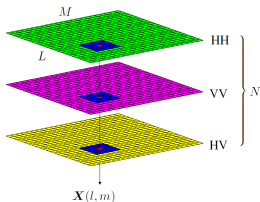


## Problem Formulation

1/2

A multipolarization SAR sensor measures for each pixel of the image under test  $N \in \{2, 3\}$  complex returns, collected from different polarimetric channels.

The  $N$  returns from the same pixel are stacked to form the vector  $\mathbf{X}(l, m)$ , where  $l = 1, \dots, L$  and  $m = 1, \dots, M$ .



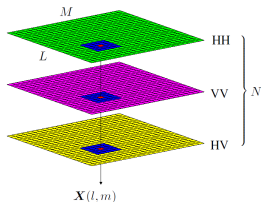
- We suppose that  $\mathbf{X}$  (reference data) and  $\mathbf{Y}$  (test data) of the same geographic area are available;

## Problem Formulation

1/2

A multipolarization SAR sensor measures for each pixel of the image under test  $N \in \{2, 3\}$  complex returns, collected from different polarimetric channels.

The  $N$  returns from the same pixel are stacked to form the vector  $\mathbf{X}(l, m)$ , where  $l = 1, \dots, L$  and  $m = 1, \dots, M$ .



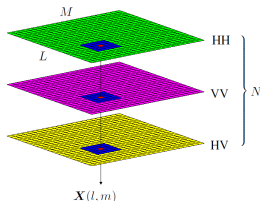
- We suppose that  $\mathbf{X}$  (reference data) and  $\mathbf{Y}$  (test data) of the same geographic area are available;
- We focus on the problem of detecting the presence of possible changes in a rectangular neighbourhood  $\mathcal{A}$ , with size  $K = W_1 \times W_2 \geq N$ , of a given pixel;

## Problem Formulation

1/2

A multipolarization SAR sensor measures for each pixel of the image under test  $N \in \{2, 3\}$  complex returns, collected from different polarimetric channels.

The  $N$  returns from the same pixel are stacked to form the vector  $\mathbf{X}(l, m)$ , where  $l = 1, \dots, L$  and  $m = 1, \dots, M$ .



- We suppose that  $\mathbf{X}$  (reference data) and  $\mathbf{Y}$  (test data) of the same geographic area are available;
- We focus on the problem of detecting the presence of possible changes in a rectangular neighbourhood  $\mathcal{A}$ , with size  $K = W_1 \times W_2 \geq N$ , of a given pixel;
- We denote by  $\mathbf{R}_X$  ( $\mathbf{R}_Y$ ) the matrix whose columns are the vectors of the polarimetric returns from the pixels of  $\mathbf{X}$  ( $\mathbf{Y}$ ) which fall in the region  $\mathcal{A}$  and  $\mathbf{S}_X = \mathbf{R}_X \mathbf{R}_X^\dagger$  ( $\mathbf{S}_Y = \mathbf{R}_Y \mathbf{R}_Y^\dagger$ ).



## Problem Formulation

2/2

- $\mathbf{R}_X$  and  $\mathbf{R}_Y$  are modeled as statistically independent random matrices;

## Problem Formulation

2/2

- $\mathbf{R}_X$  and  $\mathbf{R}_Y$  are modeled as statistically independent random matrices;
- The columns of  $\mathbf{R}_x$  ( $\mathbf{R}_y$ ) are assumed statistically i.i.d. random vectors drawn from a complex circular zero-mean Gaussian distribution with positive definite covariance matrix  $\boldsymbol{\Sigma}_X$  ( $\boldsymbol{\Sigma}_Y$ ), complying with the structure introduced in [Novak 1990]

$$\boldsymbol{\Sigma}_X \in \Xi \quad (\boldsymbol{\Sigma}_Y \in \Xi),$$

where

$$\Xi = \left\{ \boldsymbol{\Sigma} \in \mathcal{H}_N^{++} : \boldsymbol{\Sigma} = \begin{pmatrix} \boldsymbol{\Sigma}_1 & \mathbf{0} \\ \mathbf{0} & \sigma^2 \end{pmatrix} \right\},$$

## Problem Formulation

2/2

- $\mathbf{R}_X$  and  $\mathbf{R}_Y$  are modeled as statistically independent random matrices;
- The columns of  $\mathbf{R}_x$  ( $\mathbf{R}_y$ ) are assumed statistically i.i.d. random vectors drawn from a complex circular zero-mean Gaussian distribution with positive definite covariance matrix  $\boldsymbol{\Sigma}_X$  ( $\boldsymbol{\Sigma}_Y$ ), complying with the structure introduced in [Novak 1990]

$$\boldsymbol{\Sigma}_X \in \Xi \quad (\boldsymbol{\Sigma}_Y \in \Xi),$$

where

$$\Xi = \left\{ \boldsymbol{\Sigma} \in \mathcal{H}_N^{++} : \boldsymbol{\Sigma} = \begin{pmatrix} \boldsymbol{\Sigma}_1 & \mathbf{0} \\ \mathbf{0} & \sigma^2 \end{pmatrix} \right\},$$

- In this way, the change detection problem in the region  $\mathcal{A}$  can be formulated in terms of the following binary hypothesis test

$$\begin{cases} H_0 : \boldsymbol{\Sigma}_X = \boldsymbol{\Sigma}_Y \\ H_1 : \boldsymbol{\Sigma}_X \neq \boldsymbol{\Sigma}_Y \end{cases}$$



# Unstructured and Structured GLRT

# Unstructured and Structured GLRT

1/3

- The Unstructured GLRT does not exploit the special structure of  $\Sigma_X$  and  $\Sigma_Y$  and was derived in [Novak 2005]

$$\frac{\det^2(\mathbf{S}_X + \mathbf{S}_Y)}{\det(\mathbf{S}_X) \det(\mathbf{S}_Y)} \underset{H_0}{\overset{H_1}{>}} T_U,$$

# Unstructured and Structured GLRT

1/3

- The Unstructured GLRT does not exploit the special structure of  $\mathbf{\Sigma}_X$  and  $\mathbf{\Sigma}_Y$  and was derived in [Novak 2005]

$$\frac{\det^2(\mathbf{S}_X + \mathbf{S}_Y)}{\det(\mathbf{S}_X) \det(\mathbf{S}_Y)} \underset{H_0}{\overset{H_1}{>}} T_U,$$

- In our approach we consider the special structure of the covariance  $\mathbf{S}_X$  and  $\mathbf{S}_Y$

$$\mathbf{S}_X = \begin{bmatrix} \mathbf{S}_{X,1} & \mathbf{S}_{X,2} \\ \mathbf{S}_{X,2}^\dagger & \widehat{\sigma^2}_{X,1} \end{bmatrix} \quad \mathbf{S}_Y = \begin{bmatrix} \mathbf{S}_{Y,1} & \mathbf{S}_{Y,2} \\ \mathbf{S}_{Y,2}^\dagger & \widehat{\sigma^2}_{Y,1} \end{bmatrix},$$

## Unstructured and Structured GLRT

2/3

- Exploiting the Gaussian assumption together with the structure of  $\mathbf{S}_X$  and  $\mathbf{S}_Y$  the the joint probability density function (pdf) of  $\mathbf{R}_X$  and  $\mathbf{R}_Y$  can be written;

# Unstructured and Structured GLRT

2/3

- Exploiting the Gaussian assumption together with the structure of  $\mathbf{S}_X$  and  $\mathbf{S}_Y$  the joint probability density function (pdf) of  $\mathbf{R}_X$  and  $\mathbf{R}_Y$  can be written;
- The structured GLRT is the decision rule

$$\frac{\max_{\Sigma_{X,1}, \Sigma_{Y,1}, \sigma_{X,1}^2, \sigma_{Y,1}^2} f_{\mathbf{R}_X, \mathbf{R}_Y}(\mathbf{R}_X, \mathbf{R}_Y | H_1, \Sigma_{X,1}, \Sigma_{Y,1}, \sigma_{X,1}^2, \sigma_{Y,1}^2)}{\max_{\Sigma_{X,1}, \sigma_{X,1}^2} f_{\mathbf{R}_X, \mathbf{R}_Y}(\mathbf{R}_X, \mathbf{R}_Y | H_0, \Sigma_{X,1}, \sigma_{X,1}^2)} \underset{H_0}{\overset{H_1}{>}} T_{S,0}.$$

# Unstructured and Structured GLRT

2/3

- Exploiting the Gaussian assumption together with the structure of  $\mathbf{S}_X$  and  $\mathbf{S}_Y$  the the joint probability density function (pdf) of  $\mathbf{R}_X$  and  $\mathbf{R}_Y$  can be written;
- The structured GLRT is the decision rule

$$\frac{\max_{\Sigma_{X,1}, \Sigma_{Y,1}, \sigma_{X,1}^2, \sigma_{Y,1}^2} f_{\mathbf{R}_X, \mathbf{R}_Y}(\mathbf{R}_X, \mathbf{R}_Y | H_1, \Sigma_{X,1}, \Sigma_{Y,1}, \sigma_{X,1}^2, \sigma_{Y,1}^2)}{\max_{\Sigma_{X,1}, \sigma_{X,1}^2} f_{\mathbf{R}_X, \mathbf{R}_Y}(\mathbf{R}_X, \mathbf{R}_Y | H_0, \Sigma_{X,1}, \sigma_{X,1}^2)} \underset{H_0}{\overset{H_1}{>}} T_{S,0}.$$

- By replacing the unknown parameters in the likelihood ratio with their maximum likelihood estimates, under each hypothesis, we obtain the structured GLRT.

## Unstructured and Structured GLRT

3/3

- Hence, performing the maximizations over the parameters we can obtain the structured GLRT

$$\frac{\det^{2K}(\mathbf{S}_{X,1} + \mathbf{S}_{Y,1})}{\det^K(\mathbf{S}_{X,1}) \det^K(\mathbf{S}_{Y,1})} \frac{(\widehat{\sigma}^2_{X,1} + \widehat{\sigma}^2_{Y,1})^{2K}}{(\widehat{\sigma}^2_{X,1} \widehat{\sigma}^2_{Y,1})^K} \underset{H_0}{\overset{H_1}{>}} T_{S,1},$$

with  $T_{S,1}$  a modified version of  $T_{S,0}$ .

## Unstructured and Structured GLRT

3/3

- Hence, performing the maximizations over the parameters we can obtain the structured GLRT

$$\frac{\det^{2K}(\mathbf{S}_{X,1} + \mathbf{S}_{Y,1})}{\det^K(\mathbf{S}_{X,1}) \det^K(\mathbf{S}_{Y,1})} \frac{(\widehat{\sigma}_{X,1}^2 + \widehat{\sigma}_{Y,1}^2)^{2K}}{(\widehat{\sigma}_{X,1}^2 \widehat{\sigma}_{Y,1}^2)^K} \underset{H_0}{\overset{H_1}{>}} T_{S,1},$$

with  $T_{S,1}$  a modified version of  $T_{S,0}$ .

- Finally, after a monotonic transformation, we get the following equivalent form of the GLRT

$$\frac{\det^2(\mathbf{S}_{X,1} + \mathbf{S}_{Y,1})}{\det(\mathbf{S}_{X,1}) \det(\mathbf{S}_{Y,1})} \frac{(\widehat{\sigma}_{X,1}^2 + \widehat{\sigma}_{Y,1}^2)^2}{\widehat{\sigma}_{X,1}^2 \widehat{\sigma}_{Y,1}^2} \underset{H_0}{\overset{H_1}{>}} T_S,$$

with  $T_S$  the modified detection threshold.

## Unstructured and Structured GLRT

3/3

- Hence, performing the maximizations over the parameters we can obtain the structured GLRT

$$\frac{\det^{2K}(\mathbf{S}_{X,1} + \mathbf{S}_{Y,1})}{\det^K(\mathbf{S}_{X,1}) \det^K(\mathbf{S}_{Y,1})} \frac{(\widehat{\sigma}_{X,1}^2 + \widehat{\sigma}_{Y,1}^2)^{2K}}{(\widehat{\sigma}_{X,1}^2 \widehat{\sigma}_{Y,1}^2)^K} \underset{H_0}{\overset{H_1}{>}} T_{S,1},$$

with  $T_{S,1}$  a modified version of  $T_{S,0}$ .

- Finally, after a monotonic transformation, we get the following equivalent form of the GLRT

$$\frac{\det^2(\mathbf{S}_{X,1} + \mathbf{S}_{Y,1})}{\det(\mathbf{S}_{X,1}) \det(\mathbf{S}_{Y,1})} \frac{(\widehat{\sigma}_{X,1}^2 + \widehat{\sigma}_{Y,1}^2)^2}{\widehat{\sigma}_{X,1}^2 \widehat{\sigma}_{Y,1}^2} \underset{H_0}{\overset{H_1}{>}} T_S,$$

with  $T_S$  the modified detection threshold.

- It can be proved that this decision rule ensures the CFAR property with respect to both  $\Sigma_{X,1}$  and  $\sigma_{X,1}^2$ .



# Performance Assessment



## Performance Assessment

1/8

- The standard ROCs are computed for the unstructured and structured GLRTs and compared with the benchmark performance of the optimum Neyman-Pearson detector;

# Performance Assessment

1/8

- The standard ROCs are computed for the unstructured and structured GLRTs and compared with the benchmark performance of the optimum Neyman-Pearson detector;
- The optimum receiver assumes that the actual covariance matrices are known, and can be expressed as:

$$\text{tr} \left[ \left( \boldsymbol{\Sigma}_X^{-1} - \boldsymbol{\Sigma}_Y^{-1} \right) \mathbf{S}_Y \right] \underset{H_0}{\overset{H_1}{>}} T,$$

which resorting to the special structure of  $\boldsymbol{\Sigma}_X$  and  $\boldsymbol{\Sigma}_Y$  leads to

$$\text{tr} \left[ \left( \boldsymbol{\Sigma}_{X,1}^{-1} - \boldsymbol{\Sigma}_{Y,1}^{-1} \right) \mathbf{S}_{Y,1} + \left( \frac{1}{\sigma_{X,1}^2} + \frac{1}{\sigma_{X,2}^2} \right) \hat{\sigma}_{Y,1}^2 \right] \underset{H_0}{\overset{H_1}{>}} T.$$



## Performance Assessment

2/8

- In order to set the detection threshold, Monte Carlo simulations are used assuming  $100/P_{fa}$  independent runs. Additionally,  $10^5$  independent trials are exploited to estimate  $P_d$ ;

## Performance Assessment

2/8

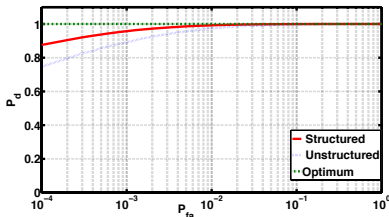
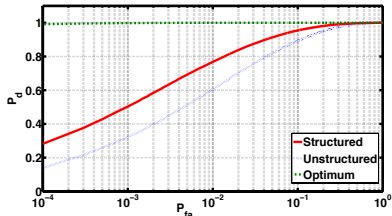
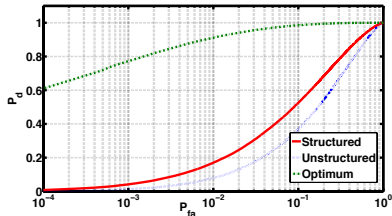
- In order to set the detection threshold, Monte Carlo simulations are used assuming  $100/P_{fa}$  independent runs. Additionally,  $10^5$  independent trials are exploited to estimate  $P_d$ ;
- The theoretical covariance matrices considered to estimate the  $P_d$  are:

$$\Sigma_X = \begin{pmatrix} 1 & 0.5 & 0 \\ 0.5 & 1 & 0 \\ 0 & 0 & 0.2 \end{pmatrix} \quad \Sigma_Y = 2\Sigma_X,$$

while  $\Sigma_Y = \Sigma_X$  was considered to estimate the  $P_{fa}$ .

# Performance Assessment

$P_d$  versus  $P_{fa}$  for  $W = [3, 5, 7]$ .



## Performance Assessment

4/8

- The analysis is performed using real X-band data available in the Coherent Change Detection Challenge dataset acquired by the Air Force Research Laboratory (AFRL).  
 The dataset has been acquired using a coherent receiver with 640 MHz bandwidth and dual-polarized mode with a range and cross-range resolution of 0.3 m;
- The selected area of interest is a sub-image of  $1000 \times 1000$  pixels (i.e.,  $L = M = 1000$ ) and is composed of several parking lots which are occupied by numerous parked, (i.e., stationary) vehicles.

# Performance Assessment

5/8

For this particular scenario the changes between the reference and test images (denoted by  $\mathbf{X}$  and  $\mathbf{Y}$  respectively), occurred during the time interval between the two acquisitions can be distinguished in two cases:

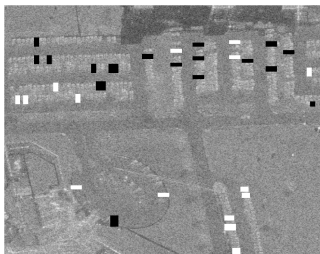
- a vehicle is present in  $\mathbf{X}$  but is not present in  $\mathbf{Y}$ , this case is referred as departure;
- a vehicle is not present in  $\mathbf{X}$  but is present in  $\mathbf{Y}$ , this event is referred as arrival.

Using the cases defined above, can be visually identified (by flickering the two images) a total of 34 changes between  $\mathbf{X}$  and  $\mathbf{Y}$ .

Reference image ( $\mathbf{X}$ )Test image ( $\mathbf{Y}$ )

## Performance Assessment

6/8



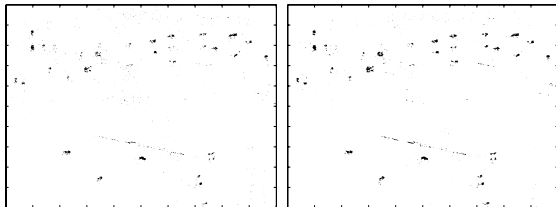
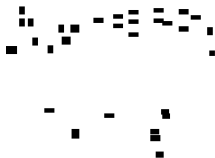
Ground truth (black regions denotes departures and white regions the arrivals) and ground truth with guard cells .

- For each detector, the thresholds are set to ensure  $P_{fa} = 10^{-3}$  in the complement of the extended ground truth area, namely, in the region where no changes occur;

# Performance Assessment

7/8

Detections maps for  $W = 3$

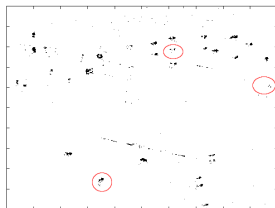
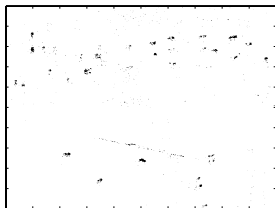


Unstructured and Structured GLRT

# Performance Assessment

7/8

Detections maps for  $W = 3$



Unstructured and Structured GLRT

# Performance Assessment

8/8

Detector	$W$		
	3	5	7
Unstructured GLRT (6)	3802	6492	7533
Structured GLRT (8)	4949	6655	7387

**Table:** Number of correct detections for  $W = 3, 5$  and  $7$ .

- The Structured GLRT outperforms the unstructured GLRT for the smaller window sizes ( $W = 3$  and  $5$ ) whereas the unstructured GLRT outperforms the structured GLRT for the larger window size of  $W = 7$  when it is able to detect more changes in the image;
- This last result can be justified in terms of a covariance model mismatch in the sense that the off-diagonal entries of the polarimetric covariance matrix which in the theoretical model have been set to zero might not be exactly zero in reality (even if very close to that value).

## Conclusions

- The block-diagonal structure for the polarimetric covariance matrix is exploited to derive a new decision rule based on the GLRT criterion;
- The proposed approach has been compared with both the optimal and the unstructured GLRT, with analysis on both simulated and real full-polarimetric SAR data;
- The performance analysis has confirmed that a structured approach can provide increase in performance with particular benefits when a small amount of homogeneous data is available;
- Possible future research tracks will consider the extension of the framework relaxing the Gaussian requirement for the data as well as the analysis on other datasets acquired by a different system, possibly at different resolutions (different performance behaviours could be observed on different datasets).



**THANKS FOR THE KIND ATTENTION**